ELSEVIER

Composites: Part B 32 (2001) 33–45

composites
Part B: engineering

www.elsevier.com/locate/compositesb

Strain monitoring in composite-strengthened concrete structures using optical fibre sensors

Kin-tak Lau[a], Chi-chiu Chan[b], Li-min Zhou[a,*], Wei Jin[b]

[a]*Department of Mechanical Engineering, The Hong Kong Polytechnic University, Hunghom, Kowloon, Hong Kong, People's Republic of China*
[b]*Department of Electrical Engineering, The Hong Kong Polytechnic University, Hunghom, Kowloon, Hong Kong, People's Republic of China*

Received 9 August 2000; accepted 7 September 2000

Abstract

In this paper, the mechanical behaviour of the composite-strengthened concrete structures is addressed. Optical fibre sensor presents a great deal of potential in monitoring the structural health condition of civil infrastructure elements after strengthening by externally bonded composite materials. The use of embedded optical fibre sensor for strain and temperature monitoring enables to reveal the status of the composite-strengthened structure in real-time remotely. In this paper, an experimental investigation on the composite-strengthened concrete structures with the embedment of fibre-optic Bragg grating (FBG) sensors is presented. Single- and multiplexed-point strain measuring techniques were used to measure strains of the structures. Frequency modulated continuous wave (FMCW) method was used to measure strains in different points of the structure with using only one single optical fibre. All strains measured from the sensors were compared to conventional surface mounted strain gauges. Experimental results show that the use of the embedded FBG sensor can measure strain accurately and provide information to the operator that the structure is subjected to debond or micro-crack failure. Multiplexed FBG strain sensors enable to measure strain in different locations by occupying only one tiny optical fibre. Reduction of strength in composite laminate is resulted if the embedded optical fibre is aligned perpendicular to the load-bearing direction of the structure.

Keywords: Optical fibre

1. Introduction

Optical fibres have been developed for long-distance data transmission in the telecommunications industry. However, in their earliest application, optical fibre was conceived as a medium for transmission of light in medical endoscopy. The use of optical fibres for applications in the telecommunications industry actually started in the mid 1960s, and ever since has gone through tremendous growth and advancement. The development of optical fibre sensors started in 1977 even though some isolated demonstrations proceeded this date [1–3]. The increased use of advanced composites in aeronautics instigated the need for new damage detection techniques, which can monitor the integrity of structural components during service period. Therefore, the optical fibre sensors have been extensively employed as real-time damage detection tools in advanced aircraft and space vehicles [4].

Recently, a strong demand on developing high performance structures, which are able to monitor the physical and mechanical properties such as temperature and strain during service condition is appreciated as a "Smart structural health monitoring system" [5]. Fibre-optic Bragg grating (FBG) sensor has been recognised as a new non-destructive evaluation (NDE) technique to suit this purpose for all structural applications [6,7]. The speciality of using FBG sensor for strain sensing application is that it is able to measure strain locally with high resolution and accuracy. As the physical size of an optical fibre is extremely small compared with other strain measuring components, it enables to be embedded into structures for determining the strain distribution without influencing the mechanical properties of the host materials [8,9].

Dewynter-Marty [10] embedded the FBG sesnor into glass fibre composite laminate to monitor thermal and residual strain properties during curing process in autoclave. Lo et al. [11] developed a single pitch FBG sensor for corrosion detection for structure served in harsh environment. Kalamkarov pointed out that the FBG sensor could be used without suffering creep problem in long term application [12]. Moreover, he also found that the embedded sensor could be sustained load in high alkaline environment with no effect on the behaviour of measurement.

* Corresponding author. Tel.: +852-2766-6663; fax: +852-236-54703.
E-mail address: mmlmzhou@polyu.edu.hk (L.-m. Zhou).

1359-8368/01/$ - see front matter
PII: S1359-8368(00)00044-5

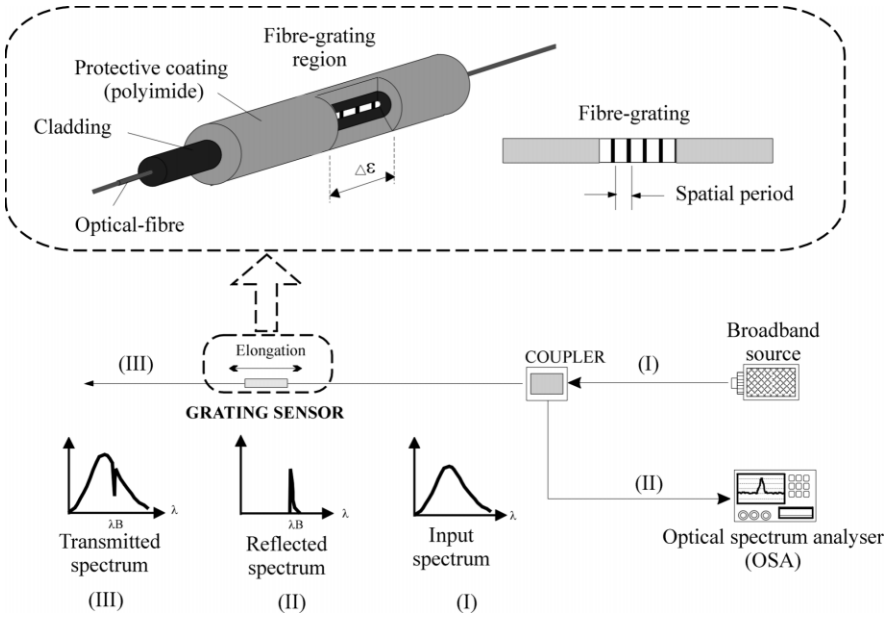

Fig. 1. FBG strain measuring system.

In this paper, experimental studies on strain measurements using embedded FBG sensors in composite, concrete and composite-strengthened concrete structures are presented. The mechanical properties of the composite laminates with the embedment of optical fibre are firstly discussed through short beam shear and flexural strength tests. The embedding technique of the sensor into concrete structure is also addressed. The FBG sensors were also embedded into the composite-strengthened concrete structure and located at the interface between concrete surface and externally bonded composites for strain measurement. Externally mounted strain gauges were used to compare results measured from the sensors.

2. Principle of FBG sensors

2.1. Strain measurement

FBG technology has been discovered by Hill et al. in 1978 [7]. It was found that the reflective grating could be photorefractively formed in the core of germanium droped silicate fibre. In general, the FBG system is comprised of broadband source (light emission device), coupler, optical spectrum analyser (OSA) and optical fibre with prewritten grating sensors. For the structural strain monitoring purpose, load is directly transferred from host material to fibre core of the grating region by the action of shear [13]. This causes the length of the grating region to be changed and the resultant refractive index of the core section to vary accordingly. The mechanical properties of the structure are simply determined by measuring the reflected wavelength change from the system. In Fig. 1, a schematic illustration of the FBG system for strain measurement is shown. Grating is written by exposing the fibre to a pair of strong Ultra-violet (UV) interference signal. This creates the grating in the core of the optical fibre, which acts essentially as a wavelength selective mirror. This method to write the grating in the optical fibre for strain and temperature measurements is called Phas mask technique (Fig. 2).

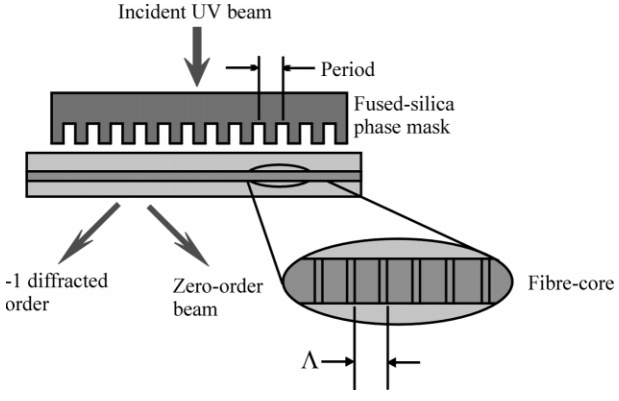

Fig. 2. Phase mask technique.

When the light is illuminated from the broadband source via the coupler, part of light is reflected back to the coupler and the reflected-wavelength is detected by the OSA as indicated in Fig. 1. The strain variation in the grating region is simply determined by the reflected wavelength shift from the sensor. According to Bragg's law, the reflective wavelength can be defined as

$$\lambda_B = 2n_{eff}\Lambda \tag{1}$$

where n_{eff} is the core refractive index and Λ is the spatial period of the index modulation. Any changes of the strain in the grating region result in changing of spatial period and core refractive index. The measurement of the mechanical

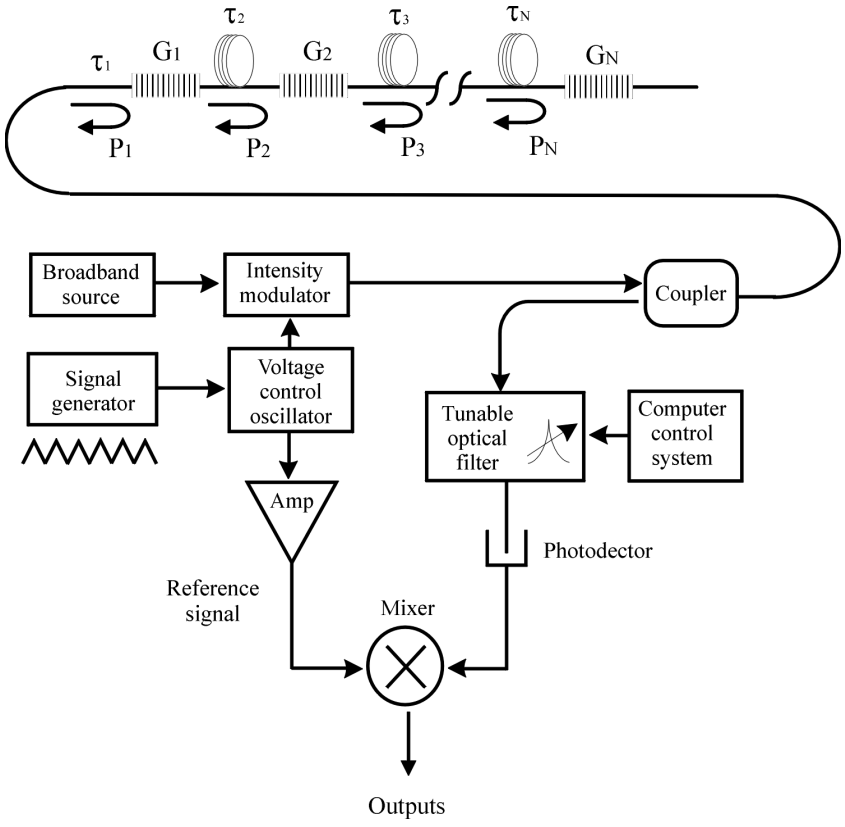

Fig. 3. Multiplexed FBG sensor arraying system by using frequency modulated continuous wave (FMCW) technique.

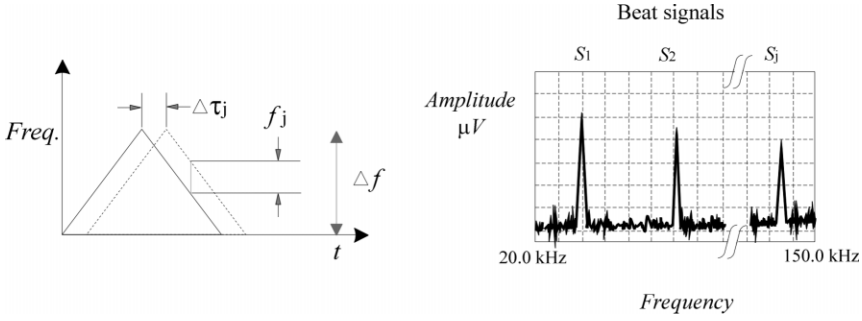

Fig. 4. The principle of the FMCW technique.

strain ($\epsilon = DL/L$) is determined by the variation of the Bragg wavelength ($\Delta\lambda_B$) shift. It has been approved that the sensors give a linear strain relationship to the reflected wavelength shift from the sensor within the elastic deformation limit of the fibre [7]. The change of the Bragg wavelength can be expressed as

$$\frac{\Delta\lambda}{\lambda_B} = \left(1 - \frac{n^2}{2}\rho_{12}\right)\epsilon_1 - \frac{n^2}{2}(\rho_{11}\epsilon_2 + \rho_{12}\epsilon_3) + \xi_0\Delta T \quad (2)$$

where ϵ_1 is the axial strain along the lengthwise direction of the fibre. ϵ_2 and ϵ_3 are the principle strains in the cross-sectional plane of the fibre core. ξ_0 is the coefficient of both the thermo-optic component and the thermal expansivity of the optical fibre, and has the nominal value of 6×10^{-6}/°C. ρ_{11} and ρ_{12} are the photoelastic coefficients. In normal, the

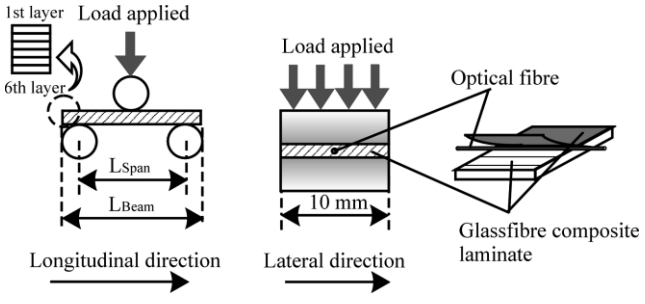

	Short beam shear test	Flexural strength test
L_{Span}	10 mm	100 mm
L_{Beam}	12 mm	120 mm

Fig. 5. Details of the composite beams for short beam shear and flexural strengths tests.

Table 1
Experimental results of the short beam shear and flexural strength tests for the optical fibre embedded glass fibre composite beam

Optical fibre	Short beam shear test (MPa)				Flexural strength test (MPa)			
	Lateral		Longitudinal		Lateral		Longitudinal	
	Mean	SD	Mean	SD	Mean	SD	Mean	SD
Sensor located at								
1st and 2nd layer	17.75	0.54	18.72	0.27	159.1	4.54	203.8	2.18
3rd and 4th layer	17.94	0.26	18.66	0.36	188.6	3.56	200.3	3.94
5th and 6th layer	18.91	0.43	18.52	0.12	190.9	3.79	198.7	2.96
No Sensor specimen	18.82	0.15	18.8	0.142	202.1	2.13	202.1	2.36

strain transfer to the fibre in transverse directions is very small and can be neglected in practical applications [14]. Therefore, the full equation for the Bragg wavelength shift by considering the effects from thermal expansion and mechanical strain of the fibre at the grating region is expressed as

$$\Delta\lambda_B = K_\epsilon \epsilon_1 + \lambda_B \xi_0 \Delta T \quad (3)$$

where K_ϵ is called "Theoretical gauge constant" [15], which can be determined experimentally. The second term in Eq. (3) represents the wavelength shift due to the temperature change in the system, which is normally used in inspecting the manufacturing process of composite materials [16]. For the silica fibre, the wavelength–strain sensitivity of 1.55 μm FBGs has been measured as 1.15 pm $\mu\epsilon^{-1}$ [17].

2.2. Multiplexing technique

One of the major advantages of using the FBG sensor in real life applications is the ability in measuring strains in different locations along structure with occupying only one single optical fibre [14,18]. This technique is normally called "Multiplexing" or "Quasi-distributed" measurement. Frequency modulated continuous wave (FMCW) technique presents it excellent ability to measure the strain variation along a single optical fibre with more than one grating sensor [19]. The FMCW offers a number of advantages compared with the current multiplexing techniques such as wavelength division (WDM) and optical time-domain reflectometry (OTDR). Typically, the maximum number of sensors that can be multiplexed by using WDM technique is about 10–12. Besides, the OTDR technique requires injecting a short pulse of optical power to the optical network and waiting for separating pulse from each sensor. It therefore requires a relatively high power in the pulse system to maintain the same average optical power at the receiving end. By using FMCW technique, it enables to produce up to 20 grating sensors along the single optical fibre if the reflectivities of the grating are correctly chosen. However, the power required is comparatively less than that by using OTDR for the same number of sensors used. Fig. 3 illustrates the multiplexed FBG sensors arraying system by using FMCW demodulating technique.

The light signal launched from the broadband source is modulated as a triangular chirped frequency carrier to the FBG sensors. The delayed frequency signal from each individual FBG sensor is returned to the tunable optical filter (TOF) and the photodetector. The detector output is

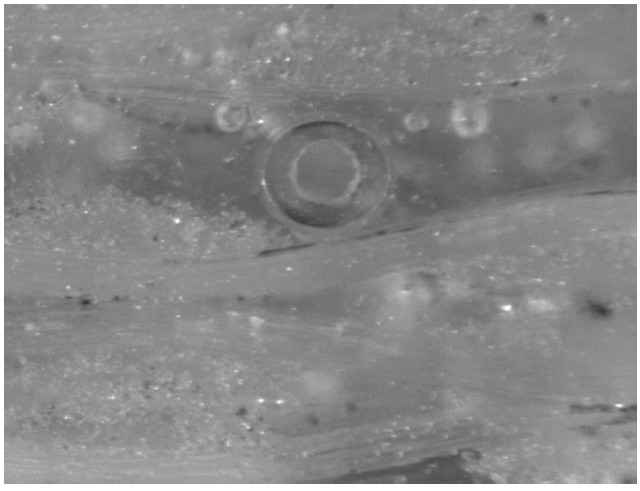

Fig. 6. Cross-sectional view of composite laminates with an embedment of optical fibre.

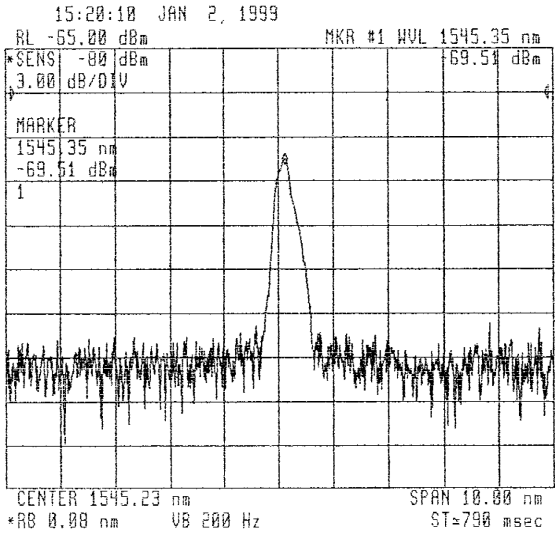

Fig. 7. Reflected wavelength spectrum from single grating sensor.

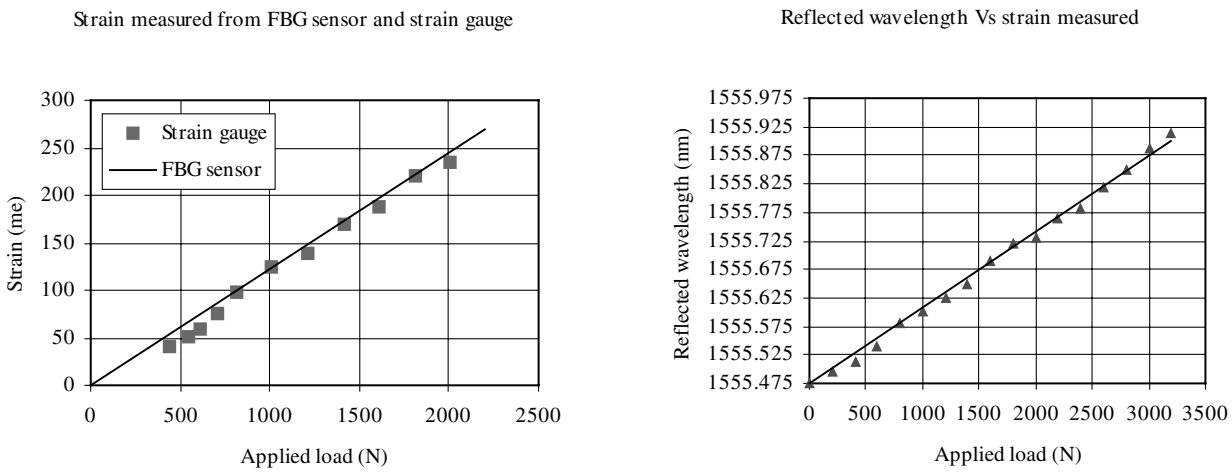

Fig. 8. Results from the sensor calibration tests.

electrically mixed with a reference chirp signal from the voltage-controlled oscillator (VCO), which produces a beat frequency associated with each sensor element. The magnitudes of the beat signals are proportional to the convolution of the individual grating reflection and the transmission spectrums of the tunable filter.

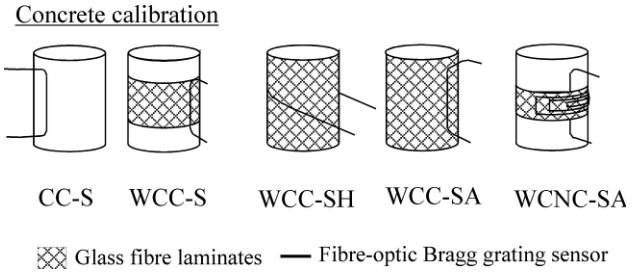

Fig. 9. Types of concrete cylinder for uni-axial compression test.

The beat signals can be viewed by using an electrical spectrum analyser (ESA). The amplitude (voltage) measured in the ESA can be converted to the corresponding strain (ϵ) of the grating. The principle of operation of the FMCW technique is illustrated in Fig. 4. The beat frequency for sensor can be expressed as

$$f_j = \Delta f \frac{\Delta T_j}{T} \tag{4}$$

where f_j, Δf, ΔT_j and T denote the beat frequency, the chirp frequency excursion, the optical delay from the source to detector for the jth sensor and the chirp period, respectively. Two major factors limit the spatial separation between two neighbouring FBG sensors. The first factor is that the separation should be long enough to avoid the coherence noise that occurs. The second one is that the separation between gratings must be large enough to separate the beat

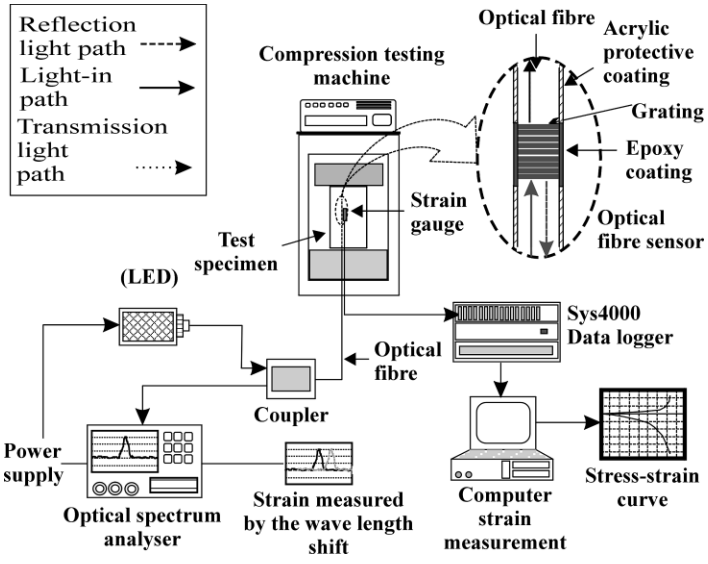

Fig. 10. Strain measuring system for the cylinder subjected to uni-axial compression test.

Table 2
Descriptions of all testing cylinders

Specimen code	Sample type	Bonding length	Direction of optical fibre
CC-S	Plain concrete cylinder	–	Axial
WCC-S	Composite-wrapped cylinder	100 mm	Axial
WCC-SH	Composite-wrapped cylinder	200 mm	Hoop
WCC-SA	Composite-wrapped cylinder	200 mm	Axial
WCNC-SA	Composite-wrapped notched cylinder	Various	Axial

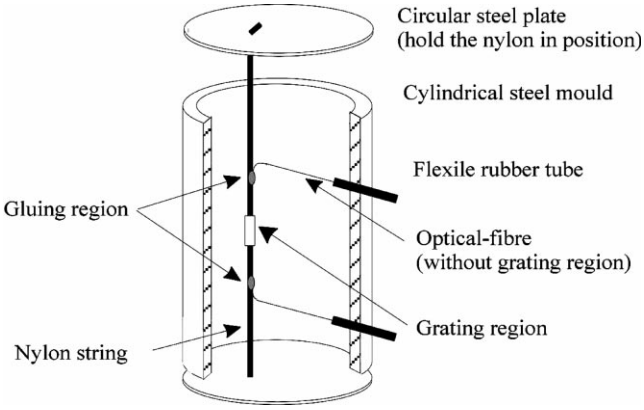

Fig. 11. Optical fibre installation technique.

signals with their frequency different between sensors and larger than the resolution of the spectral analysis techniques.

3. Strain measurement by using FBG sensors

3.1. Single grating sensor

3.1.1. Mechanical properties of glass fibre composite with the embedment of optical fibre

In the present study, the FBG sensors were used to measure strain for composite and composite-strengthened concrete structures. Since the diameter of the optical fibre ($\approx 250\ \mu m$) is relatively small compared to the concrete structure, we can assume that the mechanical properties of the structure would not be influenced by this tiny embedded optical fibre. However, for the composite structure, which is generally fabricated in a very thin cross-sectional form, the influence in mechanical strength of the structure after embedding the optical fibre becomes significant.

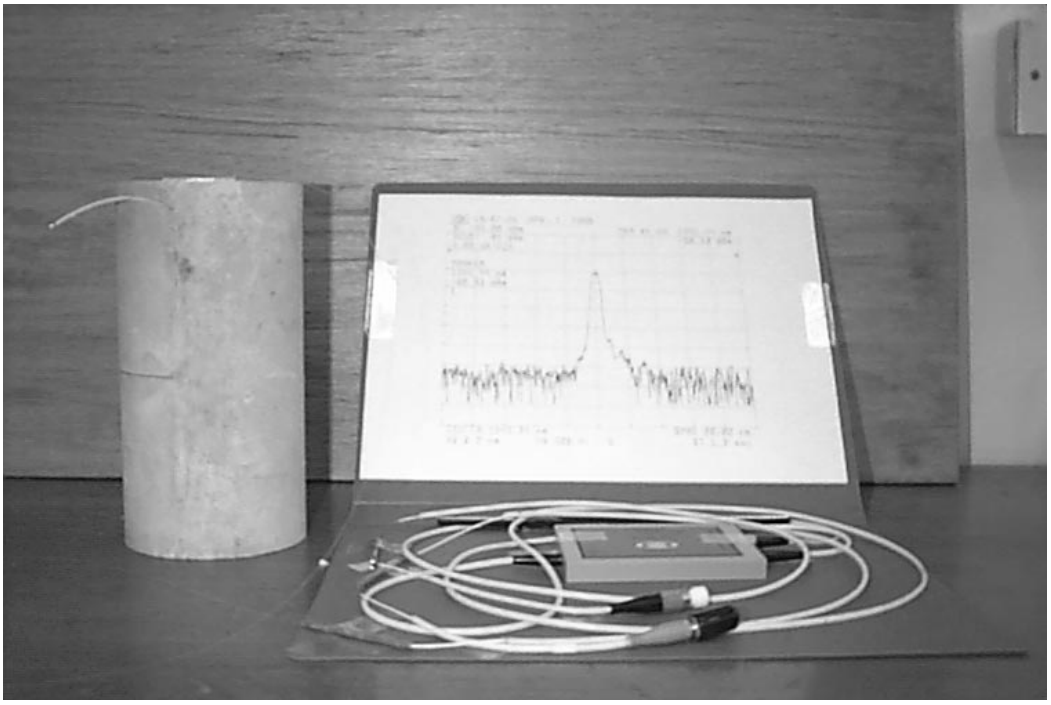

Fig. 12. Notched concrete cylinder with an embedment of FBG sensor (left) and connection to coupler (right).

Table 3
Descriptions of all strengthened beams with the embedment of FBG sensors

Code	Strengthening surface(s)	Number of layer(s)	Size of GFRP plate
SB-S1	Tension	1	250 mm × 152 mm
SB-S2	Tension	1	250 mm × 152 mm
	Shear	1	250 mm × 76.2 mm
SB-S3	Tension	6	250 mm × 152 mm (1st two layers) 200 mm × 152 mm (2nd two layers) 152 mm × 152 mm (last two layers)
	Shear	6	250 mm × 76.2 mm (1st two layers) 200 mm × 63.5 mm (2nd two layers) 152 mm × 50.8 mm (last two layers)

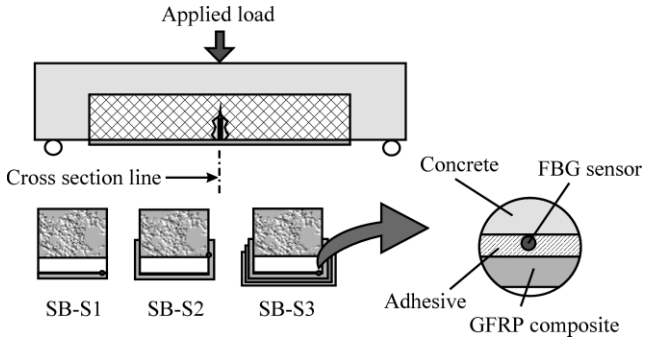

Fig. 13. Rectangular beams for three point bending test.

The short-beam shear and flexural strength tests were firstly performed to investigate the interlaminar shear and flexural strength properties of composite beams with the embedment of optical fibre. The tests followed the procedures from the ASTM D 2334 and ASTM D790. A total of 160 pieces of testing specimen were made and ten specimens for each individual test were used to ensure the reliability of the testing result. The optical fibres were aligned in both the beam longitudinal and lateral directions, and embedded in different laminate layers for the tests. In Fig. 5, a schematic diagram of the experiment illustration is shown. The results from the experiment are listed in Table 1. According to the testing results, it obviously shows that there are no significant effects to the composite structure when the optical fibre is embedded longitudinally in terms of its short beam shear and flexural strengths. The reduction of the flexural strength to 12% is resulted when the optical fibre is embedded laterally at the interface between the 1st and the 2nd layers of the glass fibre composite laminate. This may be due to the compressive buckling at the top layer of the composite laminate which occurred when the beam was subjected to bending load, resulting in a slight reduction in the short beam shear strength for the composite with the embedment of optical fibre in the lateral direction. Fig. 6 shows a cross-sectional view of the composite plate with the embedment of the optical fibre.

3.1.2. Calibration

A calibration test was performed to determine the gauge constant value as indicated in Eq. (3) for the FBG strain measuring system. Since all experiments were conducted

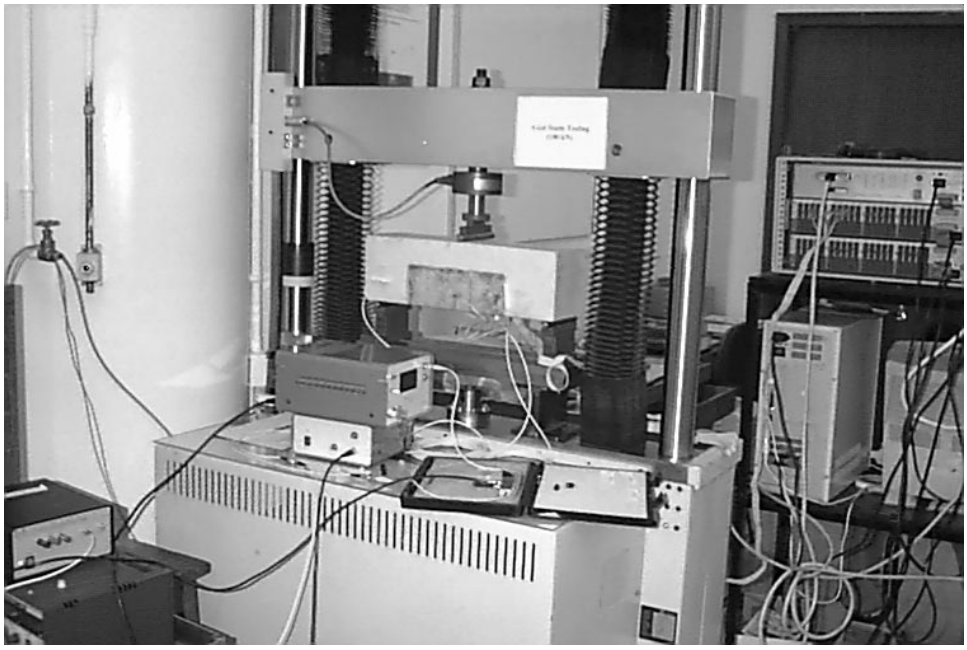

Fig. 14. Experimental set up for strain measurement in composite-bonded concrete beam.

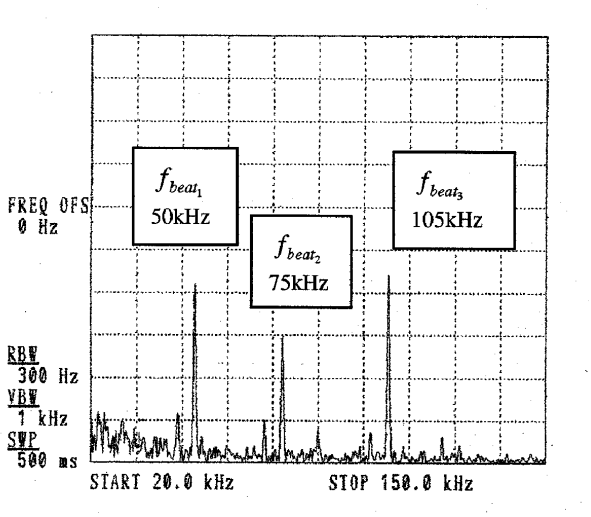

Fig. 15. Reflected wavelength spectrum for multiplexed FBG sensors.

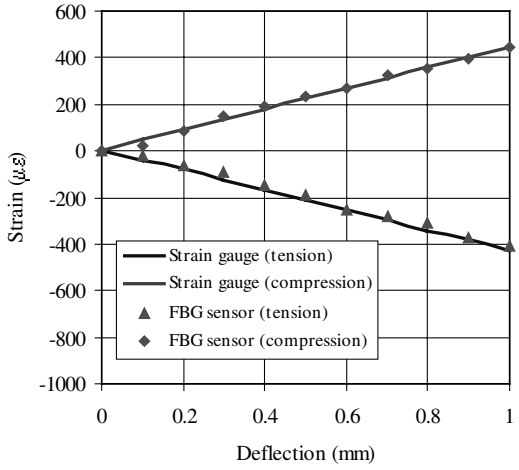

Fig. 16. Strains measured from multiplexed FBG sensors and strain gauges under four point bending test.

in temperature controlled environment, the thermal effect could be neglected in the study. A standard dog bone shape steel plate was used for a tensile strength test. An optical fibre with a grating was adhered on one side of the steel plate while strain gauge was bonded on another side to compare measuring parameters. The grating and total embedding lengths of the FBG sensor were 12 and 235 mm, respectively. The selected Bragg wavelength used was 1555 nm and the loss was less than 0.2 dB/km [20]. The spectrum captured from the OSA and experimental results during the test are plotted in Figs. 7 and 8. From the figure, the value of K^{-1} was calculated by fitting a curve as 947.55 nm^{-1}. This implies that each 947.55 nm^{-1} shift of the reflective wavelength corresponds to 1×10^{-6} strain change. Eq. (3) can be written as the reverting form

$$\epsilon_f = 947.55\lambda_B - 1473917.45. \quad (5)$$

3.1.3. Composite-wrapped concrete cylinders

The FBG sensors were installed in various forms in concrete cylinders with and without wrapping by glass fibre composite laminates. These include: (1) embedded into plain concrete cylinder (intrinsically); (2) bonded at the interface between concrete surface and glass fibre composite laminates in the directions parallel and perpendicular to the axial axis of the composite-wrapped concrete cylinder; (3) embedded into composite-wrapped notched concrete cylinder and located in front of the notch-tip. The schematic diagram of the testing specimens and experiment set up are illustrated in Figs. 9 and 10. The FBG sensors were adhered on the concrete surface by using epoxy adhesive and remained in place for 24 h. The glass fibre composite laminates were then laid-up directly on the concrete surface. Surface mounted strain gauges were used to measure surface strains of the wrapped concrete cylinder and compare the results from the internal strain measured by

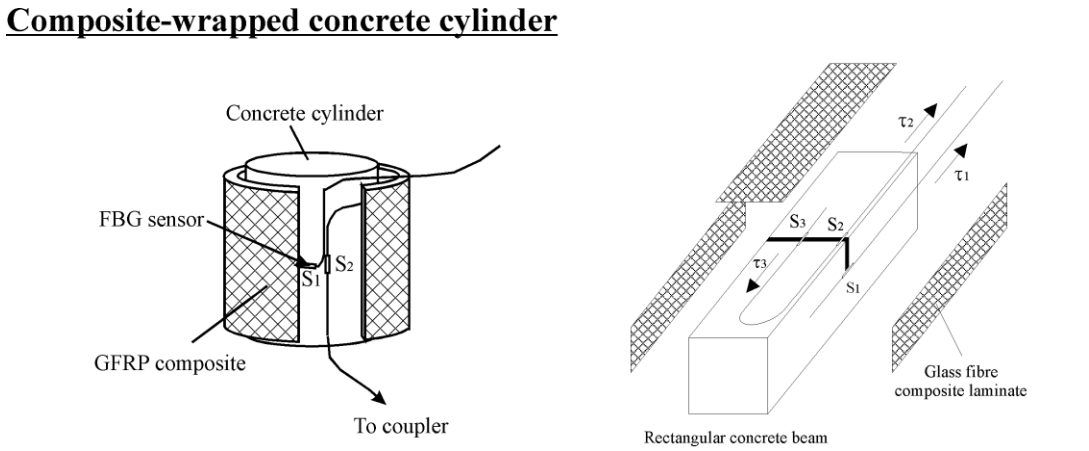

Fig. 17. Composite strengthened concrete cylinder and beam with the installation of multiplexed FBG sensors.

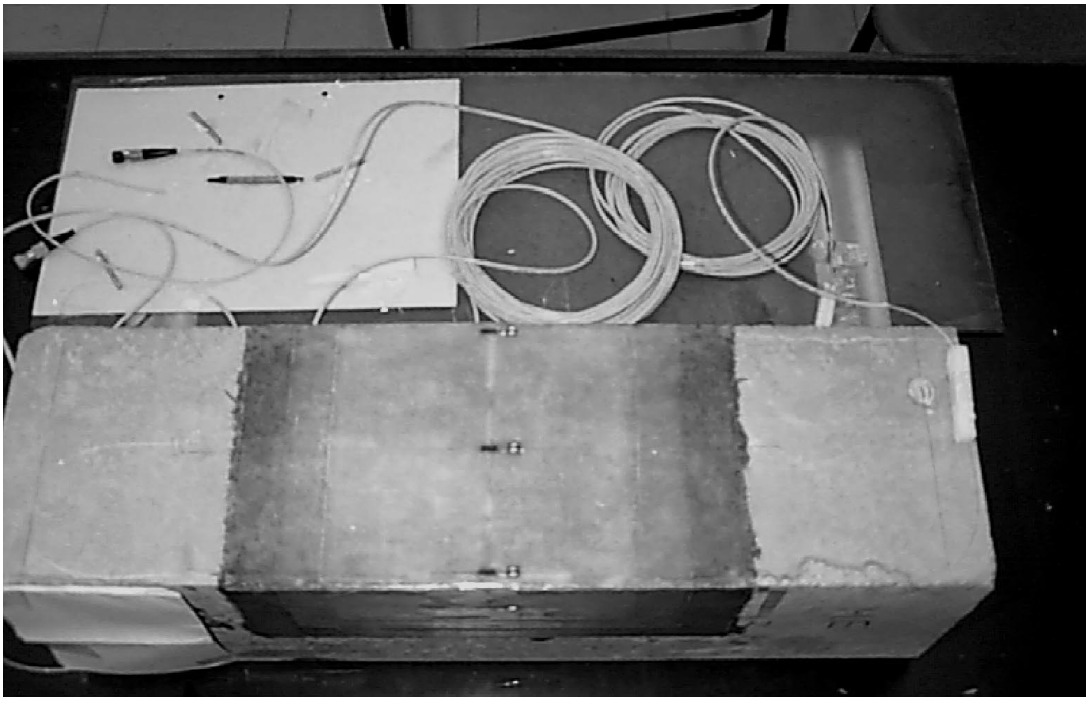

Fig. 18. Photography of the composite-bonded concrete beam for strain measurement.

the embedded FBG sensor. The descriptions of all the testing cylinders are listed in Table 2.

To avoid damage of the fibre sensor during handling and moulding processes, a special supporting fixture for aligning and reinforcing the sensor is introduced. Thin and tough nylon string was used to align and guide the optical fibre in line parallel to the load direction. Both ends of the sensor were stuck on the string by using epoxy adhesive. High flexible rubber tubes were used to protect the fibre at both entrance and exit locations of the concrete cylinder to minimise the risk of fibre breakage due to the formation of sharp turning or other unexpected damage during moulding and de-moulding processes. An illustration of the optical fibre installation technique and a photograph of the notched concrete cylinder with the optical fibre before laying-up the composites are shown in Figs. 11 and 12.

3.1.4. Composite-bonded concrete beams

Three laboratory size concrete beams with a notch formation on tension surface were used in the present study. Glass fibre composites were laid up directly on the beams by using hand lay-up method. FBG sensors were bonded either on the tension or tension and shear surfaces of the concrete beam before laying up the composites. Detailed information and schematic illustration of the testing specimens are listed in Table 3 and Fig. 13. All the beams after strengthening by composite laminates were then subjected to three point bending test. The strain measured from the embedded sensors and the externally bonded strain gauges were recorded simultaneously. The experiment set-up for the strain measurement of the composite-strengthened beam is shown in Fig. 14. The FBG strain measuring system is same as illustration, which is shown in Fig. 10 for the wrapped concrete cylinder.

3.2. Multiplexed grating sensors

The FMCW technique was used to demodulate the frequency response from multiplexed grating sensors. Three grating sensors were written into one single optical fibre to measure strains in different points of the structure. The separation of each sensor was 1 m, which was for long sufficient enough to avoid the occurrence of coherent noise,

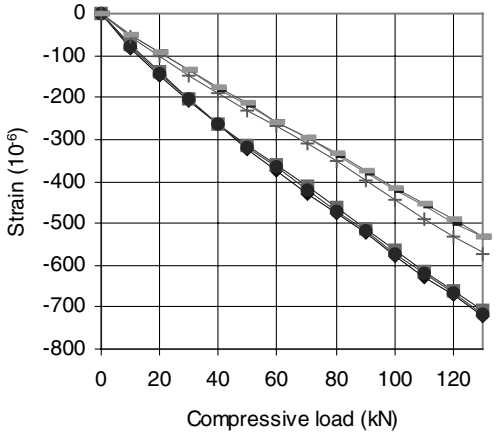

Fig. 19. Experimental result for the cylinder WCC-S (top) and CC-S (bottom). Dot and solid lines represent results measured from strain gauges and FBG sensors, respectively.

which interferes the incoming responses from the sensors inside the fibre core. The FBG sensors were embedded into 20 layers of balanced type glass fibre composite beam with a fibre volume fraction of 42%. The dimension of the beam was 235 mm (length) × 26.6 mm (width) and 3.8 mm (thickness). Two grating sensors were embedded at the interfaces between the 1st and the 2nd layer, and the 19th and the 20th layer of glass fibre composite laminates. A four point bending test was investigated to observe the responses measured from the sensors. One grating was used as a reference during measurement. Surface mounted strain gauges were attached on the top and bottom surfaces of the composite to compare results from the embedded sensors. A high radio frequency (RF) spectrum analyser of 30 Hz resolution and the rate of frequency excursion is approximate 4×10^{11} Hz^2 was used in the study. The selected wavelength and corresponding beat frequency in the experiment for the sensors S_1, S_2 and S_3 were 1556.3, 1554.24 and 1554.24 nm, and 50, 75 and 105 kHz, respectively. The beat frequencies measured in the experiment and the result of the measurement are shown in Figs. 15 and 16. The strain measured from multiplexed sensors give a very good match with the surface mounted strain gauges. This implies that the multiplexed sensors can be used with confidence.

The multiplexed sensors were used to measure strains for composite wrapped and bonded concrete structures when they were subjected to uni-axial compression and three-point bending tests, respectively.

The concrete cylinder was wrapped by five layers of glass fibre composite laminates. A single optical fibre with three grating sensors was pre-adhered on the concrete surface. Two sensors, S_1 and S_2 were adhered on the mid-height of the cylinder in both longitudinal and hoop directions to measure strains. Glass fibre composite laminates were then laid up directly on the concrete surface. Externally bonded strain gauges were used to measure strains on the composite surface and at the same locations that the sensors were embedded.

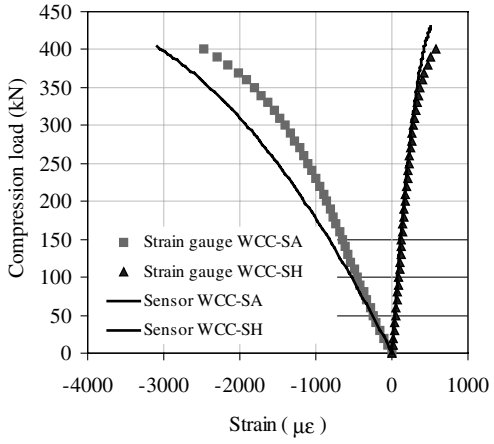

Fig. 20. Experimental results for cylinders WCC-SA and WCC-SH.

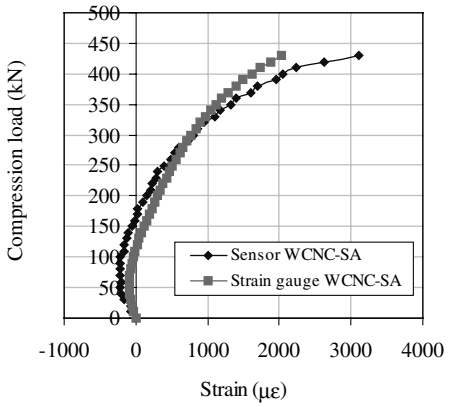

Fig. 21. Experimental results for notched concrete cylinder WCBC-SA.

For the notched rectangular concrete beam, three grating sensors were bonded on the concrete surface and at the bottom edge and centre regions, and at the notch-tip of the notched concrete beam. The sensor S_1 was located at 1 mm in front of the notch-tip, which is suspected to be highest stress area for the notched-beam without strengthening by external reinforcement. S_2 was located at the mid-beam bottom edge while S_3 was at the bottom centre and in front of the notch mouth regions. Sensors S_2 and S_3 were arrayed serially in single optical fibre and in parallel with the sensor S_1. The schematic diagrams of the composite wrapped concrete cylinder and bonded concrete beam with the embedment of multiplexed FBG sensors are shown in Figs. 17 and 18.

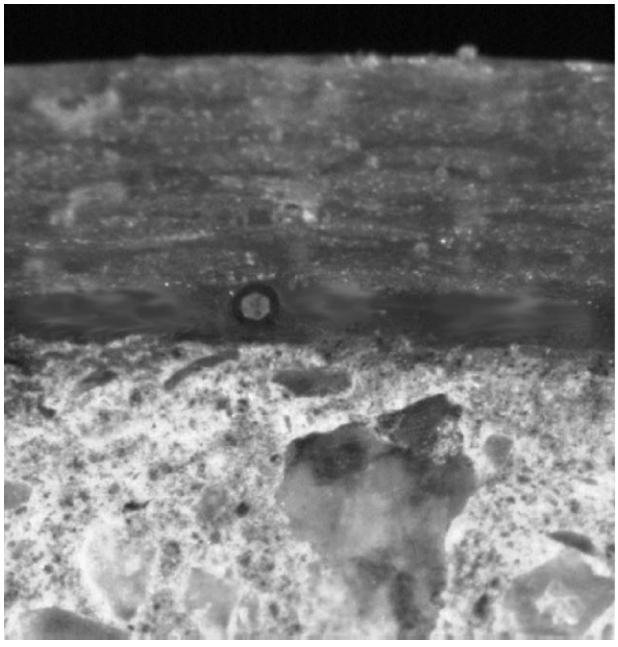

Fig. 22. Cross-sectional view of the composite-wrapped concrete cylinder with the embedment of the FBG sensor.

4. Results and discussions

Initial calibrations for the plain concrete cylinders with and without wrapping by the glass fibre composite laminates were performed. The grating sensors were located at the mid-height of the cylinder with a depth of 20 mm measured from the circumference of the cylinder surface. The specimens of CC-S and WCC-S were compressed to 1/3 of the ultimate load of the plain concrete cylinder for three repeated cycles. Surface mounted strain gauges were used to compare the results from the sensor. The experimental results are shown in Fig. 19. The results show that the internal compression strains measured from the embedded sensor well agreed with the surface mounted strain gauges at low loading range.

The experimental results for the strain measurement by using single grating sensor for the composite-wrapped concrete cylinders WCC-SH, WCC-SA and WCNC-SA are shown in Figs. 20 and 21. For the plain concrete cylinders, the compressive strains measured from the experiment give consistent reading between the FBG sensor and strain gauge when the compression load was applied to 70% of its ultimate load value. The readings are diverged when the applied load continuously increases. It is speculated that the wrapped concrete cylinder develops considerably more cracks than that for the un-wrapped concrete specimen, particularly on the concrete surface, which is located inside the wrapping region. However, the difference on the strain readings from the FBG sensor and strain gauge is large for the composite-wrapped notched-concrete cylinder at peak load condition. It was revealed that high stress was still concentrated at the notch-tip, where a sensor was embedded on the composite wrapped concrete cylinder. The properties change in this high stress concentration zone cannot be directly measured through external strain measuring device.

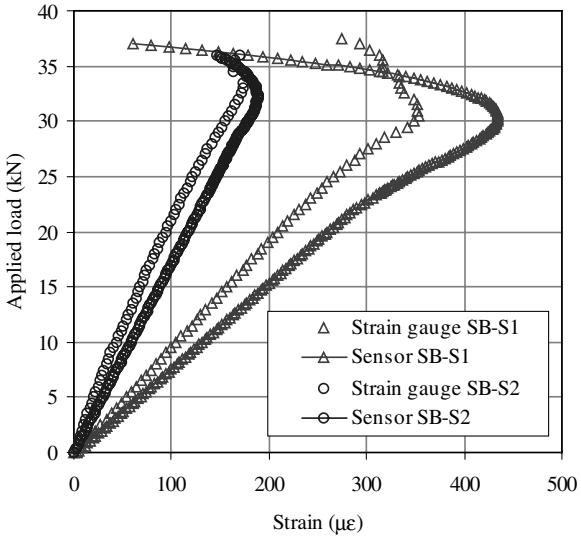

Fig. 23. Experimental results for beams SB-S1 and SB-S2.

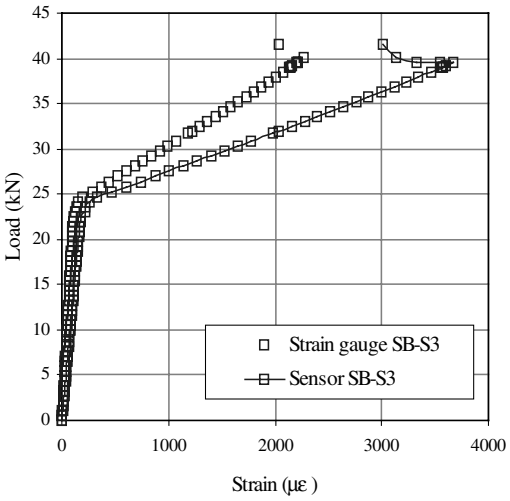

Fig. 24. Experimental result for a beam SB-S3.

In Fig. 22, a cross-sectional view of the composite wrapped concrete cylinder with the embedment of the FBG sensor is shown.

The experimental results of the strains measured from the FBG sensors and strain gauges of the specimens SB-S1, SB-S2 and SB-S3 are plotted in Figs. 23 and 24. According to the figures, it is obviously found that the strain on the concrete surface is always higher than that of the surface strain of the composite material. The FBG sensor can monitor the strain condition of the concrete and detect failure earlier than the strain gauge, which is mounted on the surface of the outer reinforcement. The result of the beam SB-S1 shows the repaid change of strains when the load is applied beyond 23 kN. During the experiment, several visible cracks and debonds were observed at adjacent areas near notch-month when the load reached 30 kN. Due to the formation of cracks, where besides the location of the sensor and strain gauge, the strain relaxation occurred when further increasing the applied load. However, this phenomenon may not influence the strain on the outer surface of the composite laminate. Therefore, the strain measured from the FBG sensor is much more sensitive to the surface crack of

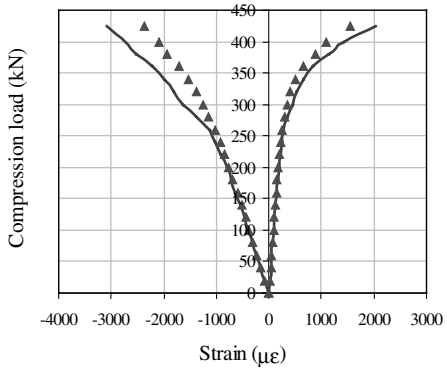

Fig. 25. Experimental results for a cylinder with embedment of multiplexed FBG sensors.

concrete and physical condition change such as debond of an adhesive layer.

For the testing specimen with the embedment of the multiplexed FBG sensors, the results are shown in Figs. 25–27. The experimental result for the composite-wrapped concrete cylinder shows that the difference of the strain measurement from the FBG sensors and strain gauges increases with increasing the applied compression load beyond 250 kN. This phenomenon implies that the axial deformation in concrete is larger than the outer surface of wrapping laminates. The differences of the strain measurement might be due to the existence of cracks on the concrete surface and high shear deformation in composite laminate (see Fig. 28). However, the divergence of the result measured in the hoop direction is relatively small when compared to the result in the axial direction since there is no shear deformation that existed in the lateral direction of the wrapping laminates.

In Figs. 26 and 27, they show that the difference of the strain measured by the externally bonded strain gauges and embedded FBG sensors increase with increasing the applied load, particularly for the sensor S_2. However, at the low loading range, the strain measured from the strain gauge and FBG sensors provide a linear load–strain relationship and give good agreement with each other in general. After the load readings to 23 kN, the divergence of the strain measurements is resulted. It was found in the experiment that high strain (5300 $\mu\epsilon$) occurred when the load was applied to 27 kN. The signal from the sensor S_2 disappeared when further increasing the applied load. It is suspected that the optical fibre was broken. The signal received from the following sensor, S_3 was therefore lost subsequently.

At the notch-tip region, the FBG sensor gave the strain response up to 31.5 kN. It was observed that the debond at the interface between the concrete and the composite laminates occurred and extended rapidly towards the opposite direction of the applied load. Shear cracking and peel-off failure were found when the applied load reached 36.5 kN. However, the surface mounted strain gauge gave a strain, which was much smaller that than the real strain measured on the concrete surface by embedded FBG sensor.

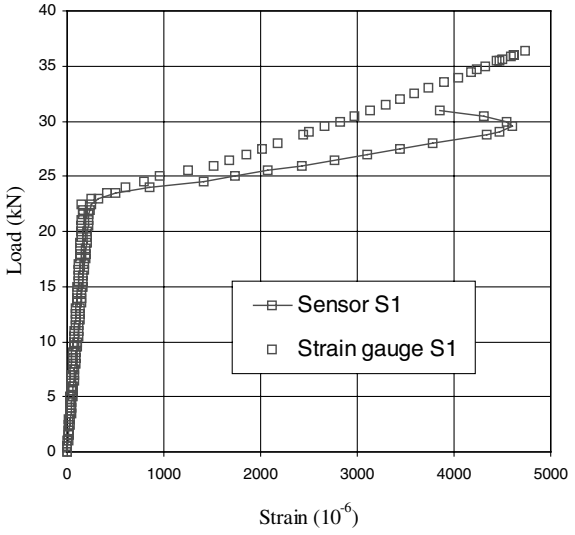

Fig. 26. Experimental result (S_1) for a beam with embedment of multiplexed FBG sensors.

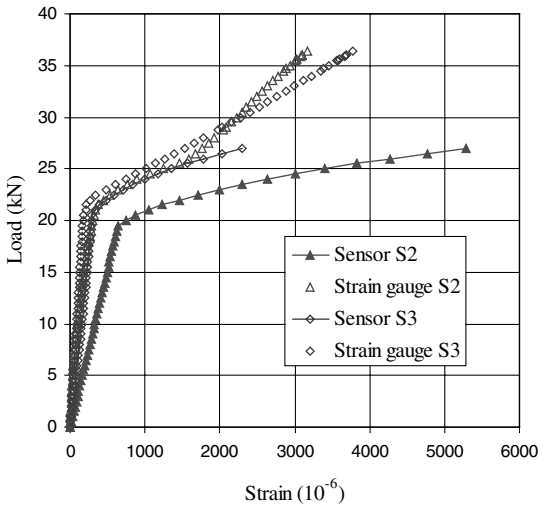

Fig. 27. Experimental results (S_2 and S_3) for a beam with embedment of multiplexed FBG sensors.

5. Conclusions

Strain measurements in composite-bonded concrete structures by using fibre-optic Bragg grating (FBG) sensors were conducted experimentally. Single and multiplexed grating sensors were used in the present study. Frequency modulated continuous wave (FMCW) technique was used to demodulate the response signals from the optical fibre with more than one grating sensor. Throughout the whole study, several conclusions can be drawn:

1. Embedded FBG sensors revealed the true strain of measurement in real time compared with externally bonded strain gauge, particularly for a structure with surface coverage reinforcement.
2. Different embedding direction of optical fibre may influence the mechanical properties of the composite structure with the embedment of optical fibre sensor. Great reduction in flexural strength of the composite structure with

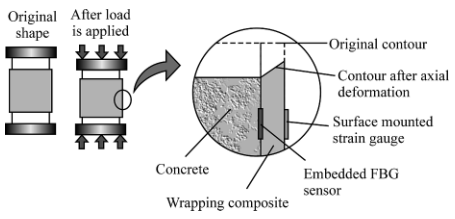

Fig. 28. Schematic illustration for composite wrapped cylinder subjected to uni-axial compression test.

the embedment of optical fibre, which orients perpendicularly to the load bearing direction.

3. Multiplexed FBG strain sensors enable to measure strains in different locations at the same time with only using one single optical fibre. In high strain condition, the properties change at the adhesive layer cannot be detected directly from the surface adhered strain-measuring devices while the FBG sensors can provide important signal to the operator.
4. The order and arrangement of the sensors is important for multiplexed strain measuring system since the sensor may loss signal if any one of the sensors, which are located in the direction from light source is broken.

Acknowledgements

This research project was funded by The Hong Kong Polytechnic Research Grant G-V528 and the Research Grant Council of Hong Kong (PolyU 5121/98E).

References

[1] Cole JH, Johnson RL, Bhuta PB. Fiber optic detection of sound. J Acoust Soc Am 1977;62:1136–8.
[2] Butter CD, Hocker GB. Fiber optic strain gauge. Appl Opt 1978;17:2867.
[3] Rutherford PS, Westerman EA. Aircraft structural integrity and smart structural health monitoring. Proc Active Mat Adapt 1992;16:267–70.
[4] Wood K, Brown T, Rogowski R, Jensen B. Fibre optic sensors for health monitoring of morphing airframe: Bargg grating strain and temperature sensor. J Smart Mater Struct 2000;9:163–9.
[5] Czarnek R, Guo YF, Bennett KD, Claus RO. Interferemetric measurements of strain concentrations induced by optical fiber embedded in a fiber reinforced composite. Proc SPIE-Int Soc Opt Engng 1989:43–54.
[6] Huang S, Ohn MM, LeBlanc M, Measures RM. Continuous arbitrary strain profile measurements with fibre Bragg grating. J Smart Mater Struct 1998;7:248–56.
[7] Maaskant R, Alavie T, Measures RM, Tadros G, Rizkalla SH, Guhathakurta A. Fibre-optic Bragg grating sensor for bridge monitoring. J Cement Concrete Compos 1997;19:21–33.
[8] Lau KT, Zhou LM, Ye L, Diao M. Investigation on upgrading and health monitoring the civil concrete structures using FRP and FBG sensor. Adv Compos Lett 1999;6(8):323–32.
[9] Lau KT, Zhou LM, Woo CH. J Mater Sci Res Int 1999;3(5):216–21.
[10] Dewynters-Marty V, Ferdinand P, Bourasseau S, Dupont M, Balageas D. Embedded fibre Bragg grating sensors for industrial composite cure monitoring. J Intell Mater Syst Struct 1998;9:785–7.
[11] Lo YL, Xiao FY. Measurement of corrosion and temperature using a single-pitch Bragg grating fibre sensor. J Intell Mater Syst Struct 1998;9:800–7.
[12] Kalamkarov AL. Processing and evaluation of pultruded smart composites with embedded fibre optic sensors. Proceedings of the Seventh International conference on Composites Engineering, University of New Orleans, USA. B35-38.
[13] Lau KT, Yuan L, Zhou LM. Strain monitoring in FRP laminates and concrete beam using FBG sensors. J Compos Struct 2000 (in press).
[14] Udd E. Fibre optic smart structures. New York: Wiley, 1995.
[15] Saouma VE, Anderson DZ, Ostrander K, Lee B, Slowik V. Application of fibre Bragg grating in local and remote infrastructure health monitoring. J Mat Struct 1998;31:259–66.
[16] Rutherford PS, Westerman EA. Aircraft structural integrity and smart structural health monitoring. Proc Active Mat Adapt 1992;16:267–70.
[17] Morey WW, Meltz G, Glenn WH. Fibre optic Bragg grating sensors. Proc SPIE 1989;1169:98–107.
[18] Lau KT, Zhou LM, Ye L. Strain evaluation on strengthened concrete beam by using FBG sensor. Non-destructive characterisation of materials IX. Am Inst Phys, USA 1999:303–8.
[19] Chan KC, Jin W, Lau KT, Zhou LM. Multi-point strain measurement of composite-bonded concrete materials with a FMCW multiplexed FBG sensor array. J Sensor Actuator 2000;87:19–25.
[20] Miya T, Terunuma Y, Hosaka T, Miyashita. Ultimate low-loss single mode fibre at 1.55 μm. Electron Lett 1979;15:106–8.